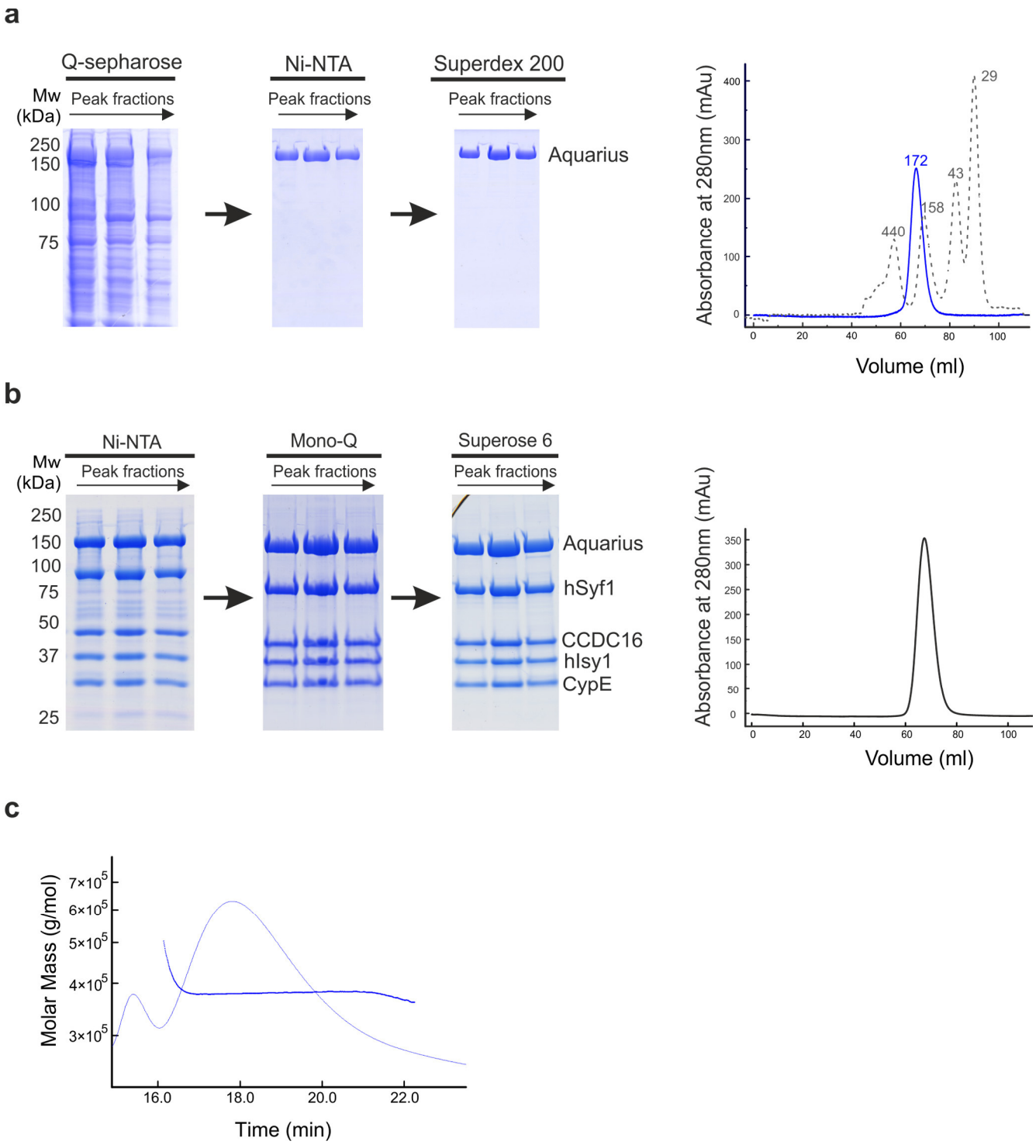

Supplementary Figure 1

Purification of recombinant Aquarius and the IBC.

Related to Figure 2. (**a**) Purification of recombinant Aquarius. SDS-PAGE analysis of the peak fractions from anion-exchange (Q-Sepharose), affinity (Ni-NTA) and size exclusion (Superdex 200) chromatography is shown on the left. The band corresponding to Aquarius is indicated. Elution profiles of Aquarius (blue line) and molecular weight standards (dashed grey line with molecular masses

in kDa) during size exclusion (Superdex 200) chromatography are shown on the right.

(**b**) Purification of the recombinant IBC. SDS-PAGE analysis of the peak fractions from affinity (Ni-NTA), anion-exchange (MonoQ) and size exclusion (Superose 6) chromatography is shown on the left. Bands corresponding to Aquarius, hSyf1, CCDC16, hIsy1 and CypE are indicated on the right. The IBC migrates as a sharp single peak in size exclusion (Superose 6) chromatography (right panel).

(**c**) Determination of the IBC's molar mass by multiangle light scattering. The molar mass *versus* the elution time is plotted. The calculated molar mass of IBC is 378 kDa.

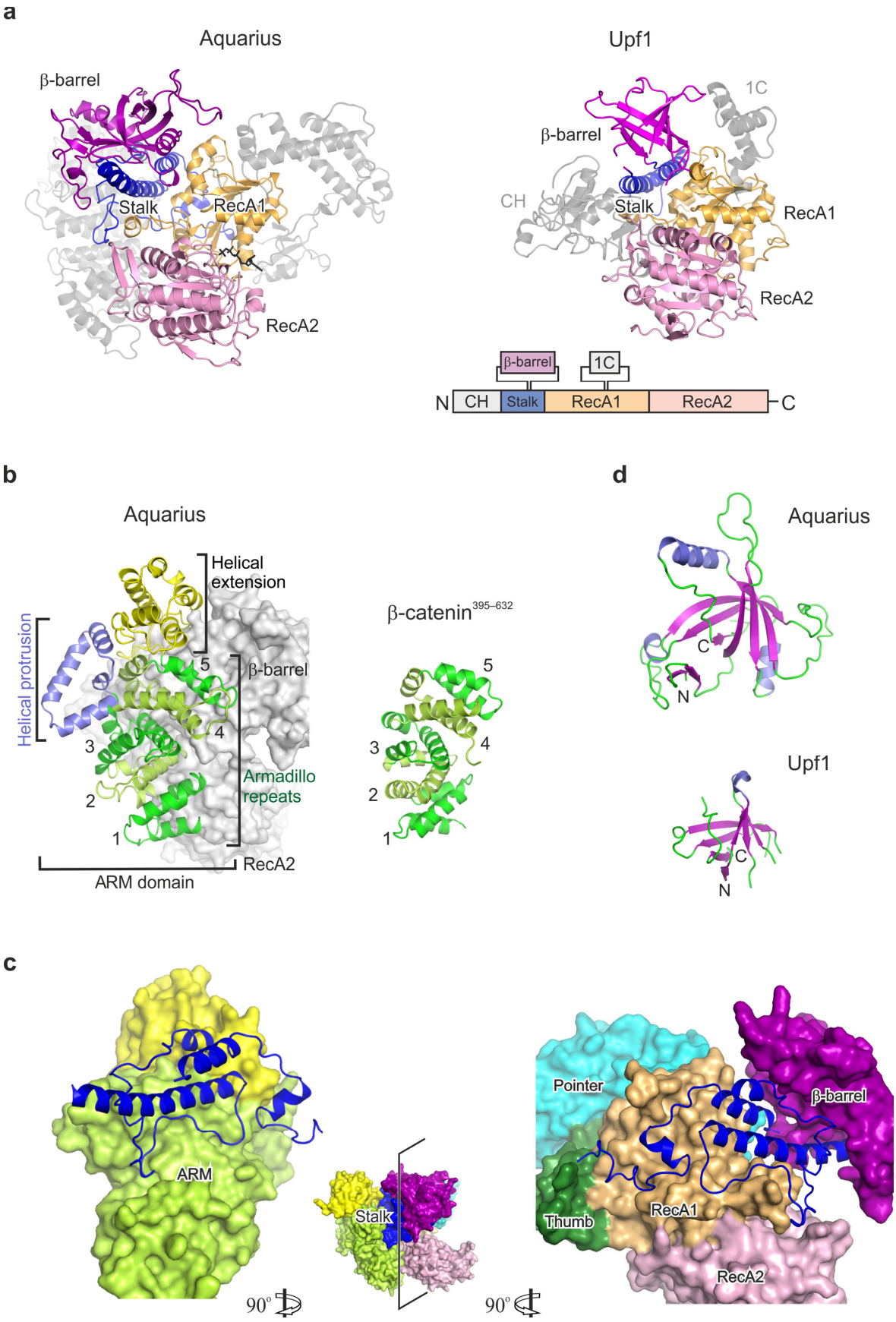
a
Aquarius
β-barrel
Stalk
RecA1
RecA2
Upf1
1C
β-barrel
CH
Stalk
RecA1
RecA2
β-barrel
1C
N
CH
Stalk
RecA1
RecA2
C
b
Aquarius
Helical extension
Helical protrusion
5
β-barrel
4
3
2
1
Armadillo repeats
RecA2
ARM domain
β-catenin395–632
5
4
3
2
1
d
Aquarius
C
N
Upf1
C
N
c
ARM
90°
Stalk
90°
Pointer
β-barrel
Thumb
RecA1
RecA2

Supplementary Figure 2

Structural features of Aquarius.

Related to Figure 1. (**a**) Structural comparison of Aquarius and Upf1 (PDB 2XZL, Chakrabarti *et al*., 2011). SF1 core domains are colored identically in both structures. Specific domains are colored grey.

(**b**) Comparison of the ARM domains of Aquarius (left) and β-catenin (right). The armadillo repeats (green and numbered), a helical protrusion (blue) and a helical extension (yellow) of the ARM domain are highlighted.

(**c**) The structure of Aquarius dissected in the middle along the stalk (blue). The two halves are rotated 90˚ either clockwise (left) or counterclockwise (right) to allow visualization of the stalk. The stalk is shown in ribbon representation.

(**d**) Comparison of the β-barrels of Aquarius (top) and Upf1 (bottom). The hydrophobic β-barrel core (magenta) is connected to helical insertions (blue) and loops (green).

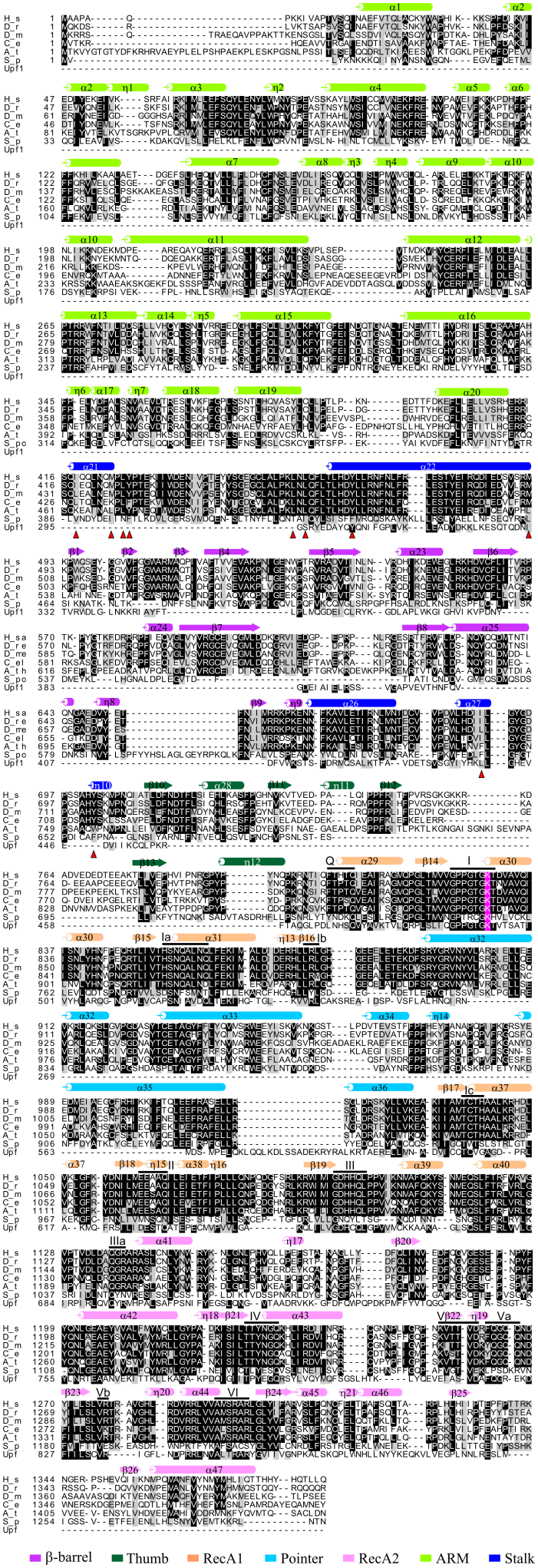

Supplementary Figure 3

Sequence alignment of Aquarius orthologs and Upf1.

The amino acid sequence of Aquarius from *Homo sapiens* (H.s.), *Danio rerio* (D.r.), *Drosophila melanogaster* (D.m.), *Caenorhabditis elegans* (C.e.) *Arabidopsis thaliana* (A.t.) and *Schizosaccharomyces pombe* (S.p.) were aligned using Clustal Omega (Sievers *et al*., 2011). The amino acid sequence of Aquarius and human Upf1 were aligned by structural superposition. The PDB access code for the latter is 2GJK. Secondary structure elements are indicated above the sequences (α – alpha helices, β – beta strands, ŋ – 3_{10} helices) and colored according to their domains (indicated at the bottom). Conserved helicase sequence motifs are indicated by black lines with Q or Roman numerals. Mutated residues are highlighted in magenta. Hydrophobic residues of the stalk involved in interactions with other domains are marked with red arrowheads.

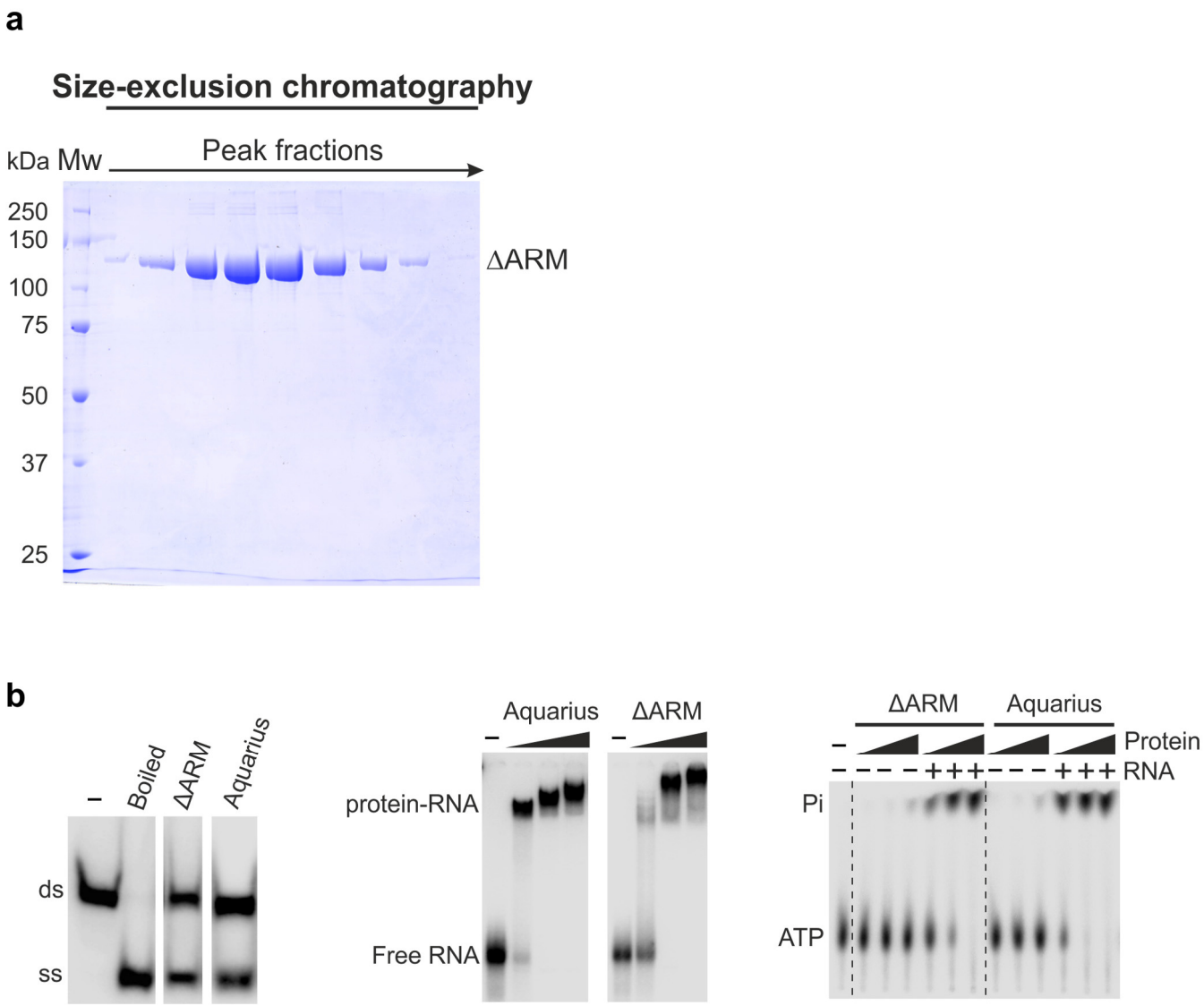

Supplementary Figure 4

Purification and biochemical characterization of Aquarius lacking an ARM domain (ΔARM).

Related to Figure 3. (**a**) SDS-PAGE analysis of the peak fractions from size exclusion chromatography of the truncated Aquarius protein (ΔARM, 417-1485). The position of the protein is indicated on the right. Molecular weight markers (Mw, kDa) are indicated on the left.

(**b**) Biochemical properties of ΔARM. Unwinding of a 3' overhang RNA duplex (left) by truncated (ΔARM) *versus* full-length Aquarius was analysed by native PAGE. The positions of double- (ds) and single-stranded (ss) RNA are indicated. RNA binding (middle) was analyzed by an electrophoretic mobility shift assay. Positions of the free RNA and protein-RNA complexes are shown. ATPase activity (right) was analysed by thin layer chromatography. The position of ATP and inorganic phosphate (Pi) are indicated.

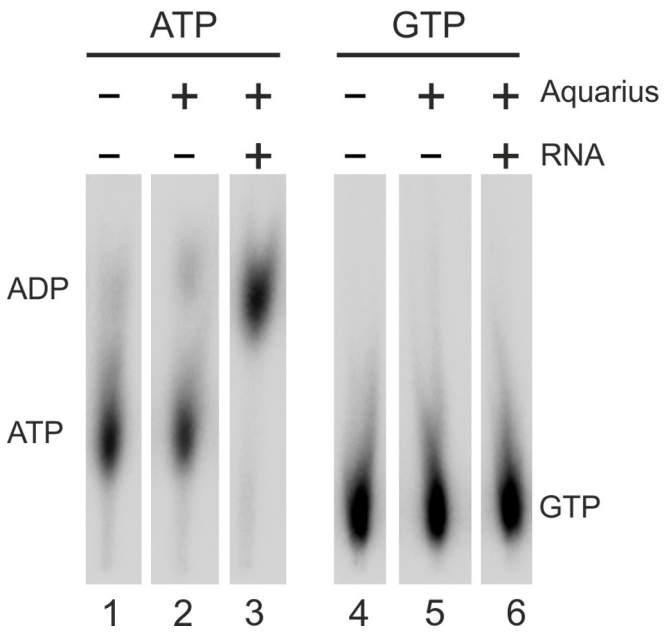

Supplementary Figure 5

Aquarius does not hydrolyze GTP.

Related to Figure 4. TLC analysis of the ATPase (lanes 1-3) and GTPase (lanes 4-6) activities of recombinant Aquarius in the presence or absence of ssRNA.

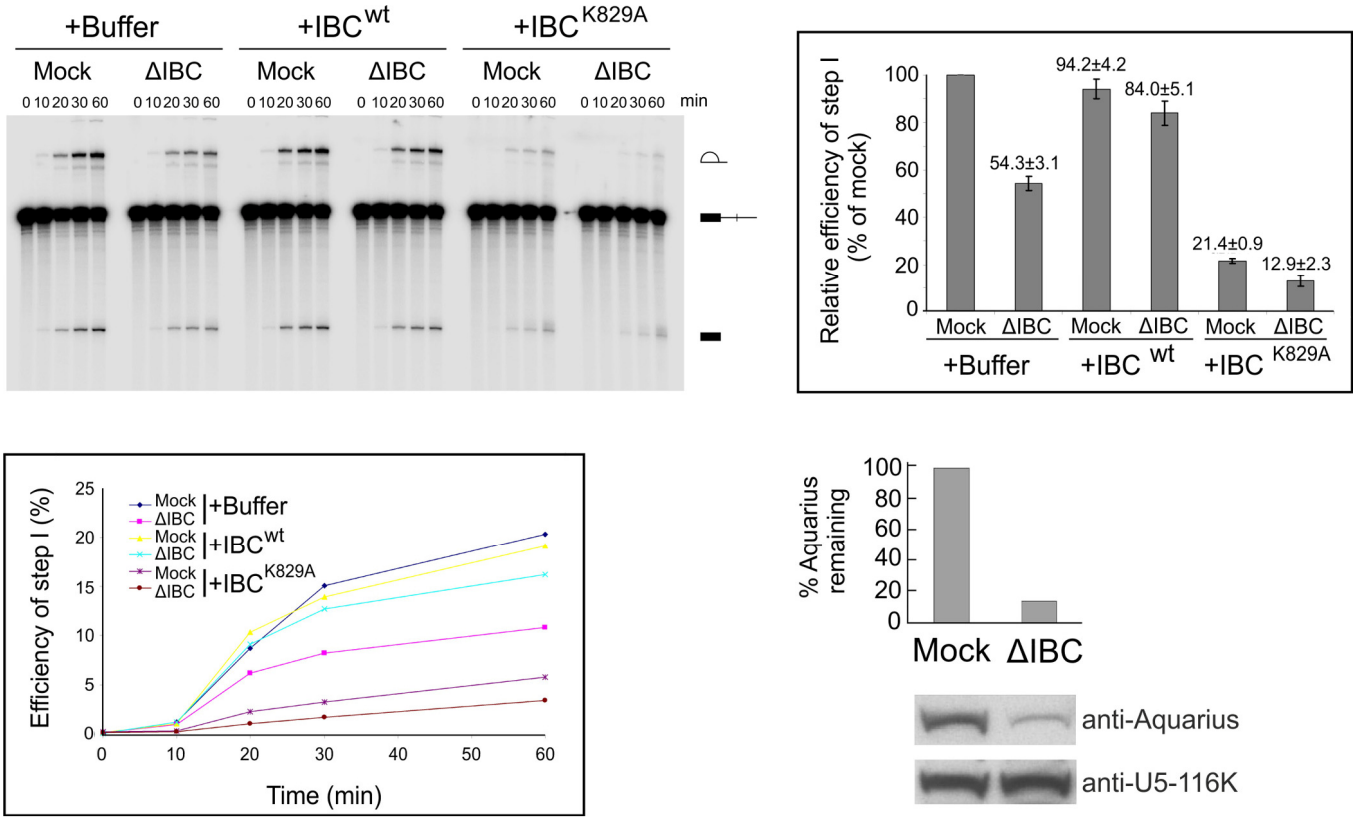

Supplementary Figure 6

Immunodepletion of Aquarius and IBC reduces splicing efficiency.

Related to Figure 6. Denaturing PAGE analysis (upper left) of splicing of PM5 pre-mRNA performed with mock-depleted or IBC immunodepleted (ΔIBC) nuclear extract in the presence or absence of purified recombinant IBC or buffer alone (as indicated above the lanes). The positions of the pre-mRNA and splicing intermediates are indicated on the right. The efficiency of the first step of splicing was calculated by dividing the sum of the intensities of the exon and intron lariat bands by the sum of the intensities of all three bands (pre-mRNA, exon, intron lariat) (bottom left). Bar diagram showing the efficiency of step I after 30 min of splicing normalized to the step I efficiency of mock-depleted extract supplemented with only buffer (set to 100%) (upper right). Values ± the standard deviation were determined from three independent experiments. The efficiency of IBC depletion was analysed by western blotting with anti-Aquarius antibodies (bottom right). Anti-U5-116K antibodies were used to demonstrate equal loading.

Supplementary Tables

Table 1. Crosslinked peptides identified within the IBC.

Protein 1	Protein 2	Peptide 1	Peptide 2	M (Th)	M (exp)
AQR (RecA2)	CCDC16	^{1245}CGNNPLIGRPN**K**VTTVDR^{1262}	^{138}IG**K**EFIR^{144}	3009.6182	3009.6192
AQR (ARM)	CCDC16	^{196}FWNLI**K**K^{202}	^{334}EILTI**K**ELQK^{343}	2299.3555	2299.3558
AQR (RecA1)	CCDC16	^{1034}IIAMTCTHAAL**K**R^{1046}	^{77}EKVAEL**K**GAK^{86}	2694.4924	2694.4813
AQR (β-barrel)	CCDC16	^{594}GCEIQGMLDD**K**GR^{606}	^{116}A**K**ATLVPQVQPSTSAWTTNFDK^{137}	4004.9612	4004.9625
AQR (thumb)	CCDC16	^{762}**K**DADVEDEDTEEAK^{775}	^{318}VE**K**LR^{322}	2374.1387	2374.1349
AQR (β-barrel)	Isy1	^{594}GCEIQGMLDD**K**GR^{606}	^{93}ELGGPDYG**K**VGPK^{105}	2931.4106	2931.4109
AQR (ARM)	Isy1	^{30}YWAPHIK**K**K^{38}	^{261}MELLQ**K**YASETLQAQSEEAR^{280}	3631.8708	3631.8737
AQR (pointer)	Syf1	^{944}WEEYIS**K**VK^{952}	^{60}AL**K**LLPCSYK^{69}	2510.3494	2510.3520
AQR (RecA1)	CypE	^{1090}WIMIGDHHQLPPVI**K**NMAFQK^{1111}	^{84}PMRI**K**EGSSR^{93}	3799.9840	3799.9956
AQR (pointer)	CypE	^{1024}S**K**YLLVK^{1030}	^{109}TLEEN**K**EEEGSEPPKAETQEGEPIAK^{134}	3855.9516	3855.9346
AQR (β-barrel)	CypE	^{594}GCEIQGMLDD**K**GR^{606}	^{115}EEEGSEPP**K**AETQEGEPIAK^{134}	3769.7298	3769.7141
AQR (RecA2)	CypE	^{1224}ISILTTYNGQ**K**HLIR^{1238}	^{84}PMRI**K**EGSSR	3053.6807	3053.6880

Table 2. Crosslinked peptides identified between the IBC and other spliceosomal proteins within the B^{act} complex.

Protein 1	Protein 2	Peptide 1	Peptide 2	M (Th)	M (exp)
SF3a120	CypE	^{1}-PAGPVQAVPPPPPVPTEPK^{20}	^{218}KFDDENFILK^{226}	3279.7430	3279.7431
CypE	SF3a66	^{79}VNLAKPMR^{86}	^{86}AAKEAK^{91}	1683.9656	1683.9541
SF3b130	CCDC16	^{977}LLRKCENK^{984}	^{340}ELQKK^{344}	1844.0504	1844.0551
SF3b130	Isy1	^{295}TKSMFFFLAQTEQGDIFK^{312}	^{106}MLDHEGKEVPGNR^{118}	3757.8434	3757.8493
SF3b155	AQR	^{478}LLVDVDESTLSPEEQKERK^{496}	^{183}LELELKK^{189}	3225.7546	3225.7636
U2A’	SyF1	^{194}GGPSPGDVEAIKNAIANASTLAEVER^{219}	^{1}VVMAR^{5}	3277.6975	3277.6935
U2A’	Isy1	^{193}KGGPSPGDVEAIKNAIANASTLAEVER^{219}	^{259}MELLQKYASETLQAQSEEAR^{280}	5155.5982	5156.5920